

# The Thermal Agitated Phase Transitions on the Ti<sub>32</sub> Nanocluster: a Molecular Dynamics Simulation Study

Tshegofatso M. Phaahla<sup>a</sup> , Alexey A. Sokol<sup>b</sup> , Charles R.A. Catlow<sup>a,b</sup> , Scott M. Woodley<sup>b</sup> ,  
Phuti E. Ngoepe<sup>a</sup>  and Hasani R. Chauke<sup>a,\*</sup> 

<sup>a</sup>Materials Modelling Centre, University of Limpopo, Private Bag X1106, Sovenga, 0727, South Africa.

<sup>b</sup>University College London, Kathleen Lonsdale Materials Chemistry, Department of Chemistry, 20 Gordon Street, London WC1H 0AJ, United Kingdom.

Received 16 April 2020, revised 2 August 2021, accepted 29 September 2021.

## ABSTRACT

Molecular dynamics simulations were performed to investigate the stability with respect to increasing the simulated temperature from 300 to 2400 K of an isolated cluster composed of 32 titanium atoms. The interatomic interactions were modelled using Gupta potentials as implemented within the classical molecular dynamics simulation software DL\_POLY. The radial distribution functions (RDF), diffusion coefficient, and density profiles were examined to study the structural changes as a function of temperature. It was found that the Ti<sub>32</sub> nanocluster exhibits temperature structural transition. The icosahedron and pentagonal bi-pyramid structures were found to be the most dominant building block fragments. Deformation of the nanocluster was also measured by diffusion coefficient, and it was found that the Ti<sub>32</sub> are mobile above the bulk melting point. The phase transitions from solid to liquid have been identified by a simple jump in the total energy curve, with the predicted melting temperature near the bulk melting point (1941.15 K). As expected, the RDF's and density profile peaks decrease with increasing temperature.

## KEYWORDS

Molecular dynamics, titanium cluster, radial distribution functions, diffusion coefficient, mean square displacement.

## 1. Introduction

Transition metal nanoclusters have attracted extensive investigation over the past decades due to their unique properties, which lie somewhere between those of bulk and single-particle species.<sup>1</sup> They have many fascinating potential uses, including quantum computers or quantum dots, light-emitting diodes, chemical sensors and photochemical applications such as flat-panel displays.<sup>2–3</sup>

Supported nanoclusters are also widely used in catalysis as a large percentage of a nanocluster's metal atoms lie on the surface, and the configurations and electronic properties of surface atoms may differ substantially from those of the bulk.<sup>4</sup> Moreover, the thermodynamics and other properties near the melting points of metallic nanoclusters are typically very different from those observed for corresponding bulk phases, thus also driving both theoretical and experimental interest in nanoclusters.<sup>5–9</sup>

For many years, theoretical studies have been used to predict structural properties and reactivity of nanoclusters or nanoparticles, including the reduced heats of formation,<sup>10,11</sup> surface premelting,<sup>12</sup> size dependence of melting temperatures,<sup>13</sup> and solid-liquid like phases.<sup>6,14</sup> These predictions on the behaviour of the nanoclusters have also been confirmed using experiments.<sup>15,16</sup> It was further reported that the melting point strongly depends on the cluster size. However, clusters of smaller sizes do not show pronounced melting temperatures.<sup>15</sup> Moreover, classical molecular dynamics (MD) simulation<sup>17</sup> was found to be both a reliable and a standard approach used to study the phase transition of the materials. The interest in applying this approach was to gain insight into the thermal stability and melting behaviour of clusters.

Employing MD, Wang *et al.*<sup>18</sup> and Cleveland *et al.*<sup>19</sup> investigated the melting behaviour of clusters and nanowires, focusing first on the melting temperature, thermal stability and mechanical properties during the melting process; secondly, on the structural evolutions and mechanical properties during heating; and thirdly on the variation of structural characteristics and size effects with temperature. Cleveland *et al.*<sup>19</sup> reported a low temperature structural solid-solid transition, from the optimal structural motif to icosahedral structures, as a precursor to melting. Compared to the bulk phase, they predicted a lower melting temperature for nanoclusters. Moreover, a much earlier investigation of Borel<sup>20</sup> reported that the melting temperature decreases with decreasing diameter of the nanoclusters. Similarly, Wang *et al.*<sup>18</sup> found a structural transition within titanium nanowires below the melting point.

In addition to identifying the melting temperature of nanoclusters, some of the main findings include the broadening of the melting transition and the appearance of a characteristic S-shaped loop in the caloric curve.<sup>21,22,23</sup> Other studies used the potential energy distribution of atoms in nanoclusters to explain many phenomena related to the phase transition of nanoclusters. Lee *et al.*<sup>13</sup> found a new type of premelting mechanism in the Pd<sub>19</sub> nanocluster. However, Breaux *et al.*<sup>24,25</sup> reported that Ga<sub>n</sub><sup>+</sup> nanoclusters (n = 17, 20, 30–50, 55) melt at temperatures ranging from 500–800 K and bulk Ga melting at a mere 303 K.

We have previously investigated the structural evolution of Ti<sub>n</sub> (n = 2–32) ground state nanoclusters and the evolution of their electronic structure.<sup>26</sup> The ground state configurations were predicted using an evolutionary algorithm to find low energy local minima on the energy landscape defined by interatomic potentials. The atomic configurations were subsequently refined using an electronic structure approach.

The chosen global optimization was implemented within the

\* To whom correspondence should be addressed.  
E-mail: [hasani.chauke@ul.ac.za](mailto:hasani.chauke@ul.ac.za)



Knowledge Led Master Code (KLMC),<sup>27</sup> which calls external codes GULP<sup>28</sup> and FHI-aims<sup>29</sup> in order to evaluate the energy and locally optimize the configurations.

This study focuses on the characteristics of ground-state configuration predicted for the Ti<sub>32</sub> nanocluster using molecular dynamic simulation. Ti<sub>32</sub> nanocluster is formed by four interpenetrating pentagonal fragments.<sup>26</sup> It was also revealed that the 32 atom titanium nanocluster resembles a low-temperature hcp  $\alpha$ -Ti. This structure was deduced from the predicted binding energy data as the cluster evolved towards the bulk system. In the next section, we outline the technique employed to simulate the melting behaviour of the Ti<sub>32</sub> nanocluster. In section 3, we discuss the effect of temperature on the electronic and structural evolution of the 32-atom titanium nanocluster.

## 2. Methodology

The initial atomic configuration was taken from our previous study,<sup>26</sup> where a genetic algorithm was employed to predict the ground state for Ti<sub>32</sub>. The energy landscape explored in our earlier work is defined by a combination of a Born-Mayer two-body and Embedded atom method (EAM) interatomic potentials.<sup>26</sup> To properly simulate the thermodynamic properties of the Ti<sub>32</sub> nanocluster, the EAM and the Born-Mayer interatomic potentials reported by Lazauskas *et al.*<sup>26</sup> were incorporated together to express the total internal energy of pure metals in terms of Gupta potentials.<sup>30</sup> Based on the second moment approximation of tight-binding theory, the Gupta potential and ion-ion interaction are described by an electronic band and a repulsive term. The total potential of system N atoms located at positions is expressed as follows:

$$U = \sum_{i=1}^N \left\{ \sum_{j \neq i} A \exp \left[ -p \left( \frac{r_{ij}}{d} \right) - 1 \right] - \sqrt{\sum_{j \neq i} \zeta^2 \exp \left[ -2q \left( \frac{r_{ij}}{d} - 1 \right) \right]} \right\} \quad (1)$$

where the first term represents repulsive many-body and the second term represents the attractive many-body. In this approach, both terms are introduced in the exponential form,<sup>31</sup> where  $d$  is the first-neighbour distance,  $\zeta$  is an affective overlap integral between the electronic orbitals of the neighbouring atom,  $q$  and  $p$  control the decay of the exponential function related to bulk elastic constants.<sup>32</sup> The MD simulations (heating/melting process) were performed in the NVT canonical ensemble. The nanocluster was confined in a cubic unit cell (at fixed lattice parameter,  $a=b=c = 50 \text{ \AA}$ ) with periodic boundary conditions applied in the  $x$ ,  $y$ ,  $z$  directions implemented within DL\_POLY software.<sup>33</sup>

The temperature  $T$  was controlled by the Nose Hoover thermostat<sup>34</sup> with a relaxation time of 0.001 ps. The time integration of the equation of motion was performed using the velocity Verlet leapfrog algorithm.<sup>33</sup> The interatomic interactions were truncated at the cutoff radius of 4  $\text{\AA}$ .

One independent MD run was performed for 23 fixed temperatures, with 300 K as our lowest chosen temperature and 2400 K our highest. A run time of 300 ps was employed to equilibrate the cluster before collecting data for 600 ps.

## 3. Results and Discussion

### 3.1. Temperature Effect on the Ti<sub>32</sub> Nanocluster

The minimum energy cluster for Ti<sub>32</sub> is presented in Fig. 1. The snapshots of the thermally agitated Ti<sub>32</sub> nanocluster are analyzed in detail to gain more insights regarding structural transition as a function of temperature ( $T$ ). Note that the (Ti<sub>32</sub>) nanocluster shows various geometrical configurations as the temperature is increased. The dominant configurations are a triangular bi-pyramid (Ti<sub>5</sub>), an octahedron (Ti<sub>6</sub>), a pentagonal bi-pyramid (Ti<sub>7</sub>), an icosahedron (Ti<sub>13</sub>) and interpenetrating icosahedra (Ti<sub>19</sub>), as shown in Fig. 1.

The temperature dependence of the equilibrium cluster structure for Ti<sub>32</sub> is shown in Fig. 2 (see supplementary information). It was found that the configurational transitions involve distortion or displacement of atoms in the Ti<sub>32</sub> nanocluster as the temperature increases. The distortion of the Ti<sub>32</sub> nanocluster becomes more frequent from lower temperatures and increasingly severe with increasing temperature. The structural transients are shown in different colour coding as the structure of Ti<sub>32</sub> nanocluster changes as a function of temperature.

The initial configuration starts as interpenetrating icosahedra, where one of the icosahedra is replaced with an icositetrahedra geometry. The transient at 300 K has two interpenetrating icosahedral units (maroon) with two pentagonal bi-pyramids (green and blue). As the temperature increases, the atomic displacement about the initial positions increases and leads to a change in the morphology of the nanocluster at 400 K to a Ti<sub>19</sub> unit (red) interpenetrating with two pentagonal bi-pyramids, Ti<sub>7</sub> (blue and lime-green), added on the sides of the Ti<sub>19</sub>. This change may be attributed to atoms in a solid that undergo vibrations about the equilibrium position, leading to distortions of crystal nanocluster.<sup>35</sup> The transition of the nanocluster at 500 K is observed to have Ti<sub>20</sub> (blue) polyhedron interpenetrating with icosahedron (gold), triangular bi-pyramid (violet) and an atom (red) connecting the triangular pyramidal and icosahedral units or nanoclusters. At 600 K, the nanocluster transitions to a Ti<sub>19</sub> (gold) polyhedron interpenetrating with a Z13 Frank Casper polyhedron Ti<sub>14</sub> (blue) and a triangular bi-pyramid (lime-green). The effect of thermal agitation at 700 K changes the Ti<sub>32</sub> morphology into two interpenetrating Ti<sub>19</sub> (gold and blue) polyhedra with a triangular unit connected to the Ti<sub>19</sub> polyhedron described by the blue colour. At 800 K, the two Z12 Frank Casper polyhedral Ti<sub>13</sub> (green and blue) form the transient unit inter-connected to pentagonal bi-pyramid (lime-green), triangular unit (violet) and an atom (red). The Ti<sub>13</sub> nanocluster (maroon) was observed to coexist with four pentagonal bi-pyramids (blue, green, and gold) at 900 K. Two interpenetrating icosahedra (lime-green and blue) complemented by tetra-capped atoms (violet and maroon) on the sides are found to be the transient for 1000 K. The transition occurring at 1100 K leads to two icosahedra connected by dimers (black and lime-green).

Furthermore, for higher thermal agitation, these fragmentation patterns reveal the existence of a stable building block,

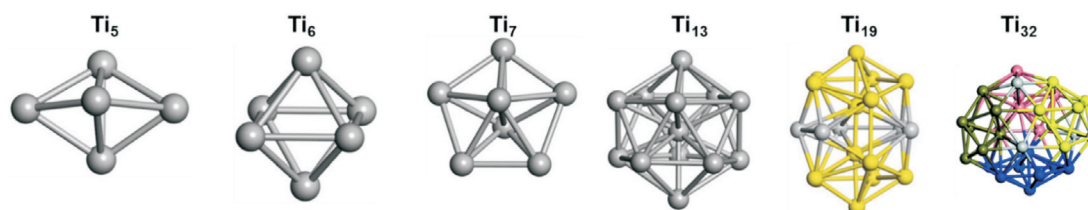


**Figure 1** Nanoclusters generated from the previous study.<sup>26</sup> (Ti<sub>5</sub> as triangular bipyramid, Ti<sub>6</sub> as octahedron, Ti<sub>7</sub> as pentagonal bi-pyramid, Ti<sub>13</sub> as icosahedron, Ti<sub>19</sub> as interpenetrating icosahedra and Ti<sub>32</sub> as four interpenetrating bi-pyramidal pentagonal fragments.)

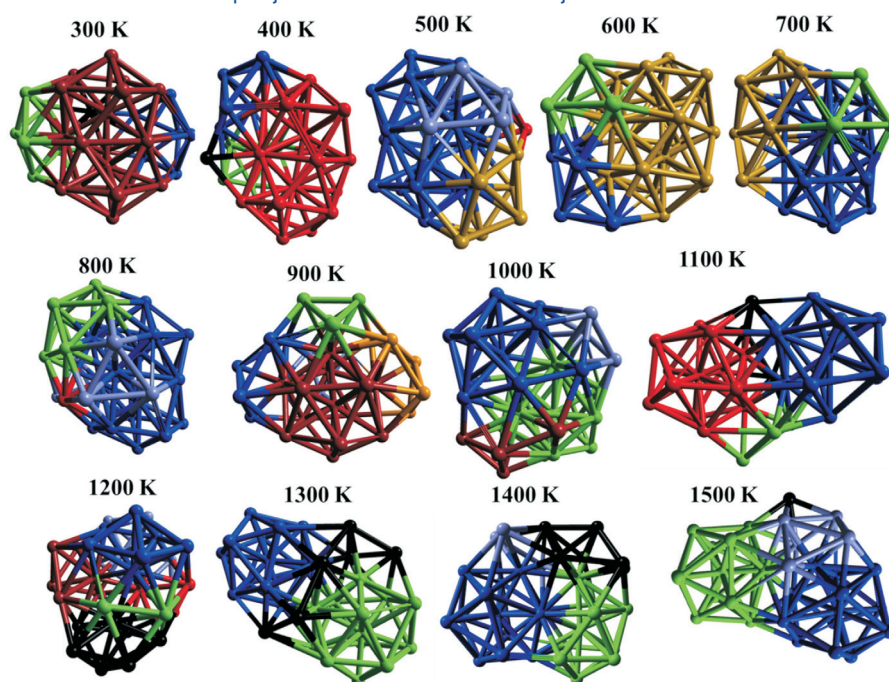


**Figure 2**  $Ti_{32}$  cluster showing a change in the morphology with increasing temperature. Subunits with different colour shades represent the structural evolution.

namely an icosahedron, or interpenetrating pentagonal bi-pyramid. At 1200, the coexistence of three-pentagonal bi-pyramid (blue, black and maroon) and triangular unit connecting all the penta-shaped units or nanoclusters with a dimer (lime-green) connecting the blue, maroon and black penta-shaped units. The transient observed for 1300 K comprises two icosahedral polyhedra (blue and lime-green) connected by six atoms. However, at 1400 K, the two interpenetrating icosahedra (blue and green) are found to coexist with a triangular bi-pyramid unit as well as a complementing dimer connecting the other fragments.

The structural transformation precursor at 1500 K is found to be two icosahedral fragments (lime-green and blue) connec-

ted by the hexagonal ring (violet, lime-green and black) or triangular bi-pyramid (violet) with an atom (black) connecting the icosahedra and triangular bi-pyramid. Furthermore, the structural transition for 1600 K, shown in Fig. 3 (see supplementary information), is noted to be two icosahedral isomers connected by triangular bi-pyramid shaped nanocluster (violet) and triangular unit (black). At 1700 K, two interpenetrating icosahedra (blue and violet) capped on top of one of the icosahedral configurations (lime-green) with an atom (black) was observed. The transient for 1800 K is found to be the icosahedron (maroon) bi-pentagonal bi-pyramid (blue and green) with tetra-coordinated capping atoms (black) completing the structure.

At 1900 K, the nanocluster transitions into three interpenetrat-

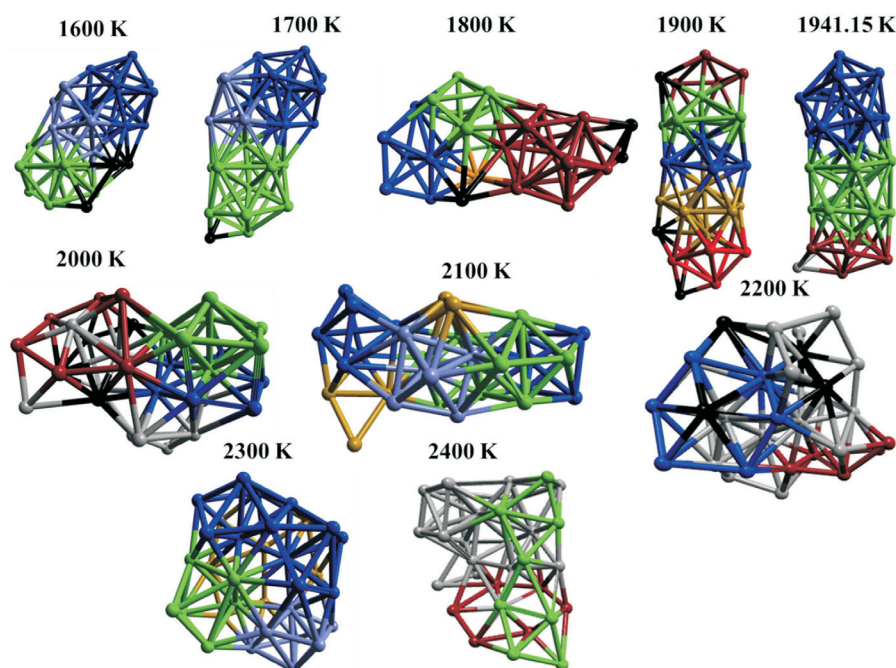


**Figure 3** Transients showing a change in morphology from 1600–2400 K. Subunits with different colour shades represent the structural evolution.

ing icosahedra capped by an atom (black), which can also be seen as four interpenetrating pentagonal bi-pyramids (lime-green, gold, blue and red) with a triangular unit (maroon) capping the top of the pentagonal bi-pyramid (lime-green) and three further single complementing atoms (black). However, at 1941.15 K, which is the melting temperature for bulk titanium,<sup>36,37</sup> the structural transition is observed to have two interpenetrating icosahedra (blue and green) capped by a pentagonal bi-pyramid (maroon) with one (grey) capping atom completing the structure. At 2000 K, three hexagonal rings (black, blue and red) coexisting with pentagonal bi-pyramid (lime-green) and additional atoms (grey) were observed.

This transition did not follow the same pattern with icosahedral dominated configurations, and the behaviour might be attributed to the configuration having a higher symmetry structure. Furthermore, at 2100 K, five octahedral isomers (lime-green, blue and violet) coexisting with eight atoms (gold and green) were observed. The 2200 K structural transition is observed to be two interpenetrating hexagonal rings (blue and black) coexisting with a pentagonal ring (maroon) and the surrounding atoms (grey). The same is observed where the nanocluster did not follow the pentagonal dominated pattern. At 2300 K and 2400 K, the thermal agitated structural transitions are to hexagonal and pentagonal shaped unit dominated configurations (blue, lime-green, violet and gold), whereas 2400 K forms a hexagonal ring (maroon) and triangular unit dominated transition. As discussed below, above 2000 K, there is appreciable atomic mobility confirming the molten state.

### 3.1.1. Heating and Cooling for $Ti_{32}$ Cluster

The melting transition of the cluster from a rigid or solid form in which atoms merely oscillate about the equilibrium structure to a liquid or fluid form characterized by atoms leaving their equilibrium basins and finding new ones with new equilibrium positions is spread over a range of temperatures from 300–2400 K. Figure 4a shows the energy varying smoothly with temperature up to 2000 K where it depicts a jump in the total energy closer to the melting temperature of bulk Ti. Thus, this behaviour may be ascribed to a solid-liquid phase transition that is in excellent agreement with the melting point of bulk Ti (1941.15 K).<sup>36</sup> This positive deviation from linearity in the total energy may be attributed to the tendency of the nanocluster undergoing surface melting.<sup>38</sup>

The most striking feature of these results is that the maximum

in the total energy occurs at a temperature above the bulk melting point. In addition, there have been theoretical reports that small nanoclusters have elevated melting temperatures.<sup>39,40</sup>

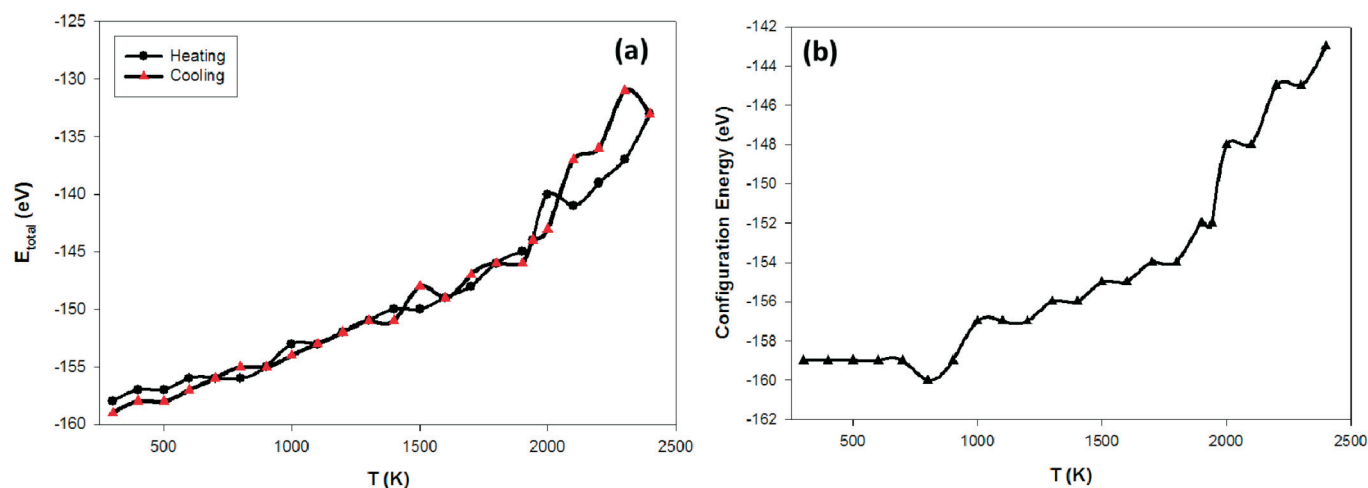
Upon cooling, the cluster undergoes a liquid-solid transition. The nanocluster energies become lower from 600–300 K, 1000 K, 1400 K, 1900 K and 2000 K, suggesting the formation of a new stable configuration. There are cooling energies higher than heating energies observed at 800 K, 1500 K, 1700 K, 2100 K, 2200 K and 2300 K, respectively, suggesting the transition to less stable configurations. The solid-liquid and liquid-solid transition have similar energies at 700 K, 900 K, 1100–1300 K, 1600 K, 1800 K and 1941.15 K suggesting similar configurations. A weak hysteresis was observed at 2000 K, suggesting a phase change accompanied by the formation of new geometry. The melting-quenching cycle discloses that it is easier for the nanocluster to go from the solid-liquid phase than the liquid-solid phase, as observed from the total energy data.

In the case of the configuration energy in Fig. 4b, it is observed that at temperatures 300–700 K, the energy is constant, followed by a dip at 800 K, which results in a lower energy nanocluster compared to other temperatures. However, a sudden jump in the energy from 800–1000 K, is followed by the linear increase from 1000–1200 K. Furthermore, a stepwise increase in energies at temperatures from 1300–2300 K is observed, with an abrupt jump in the energy at 1941.15 K that is higher than other temperatures (1900 K and 2000 K). The abrupt jump may be attributed to the phase transition of the nanocluster from a solid phase to a liquid phase.

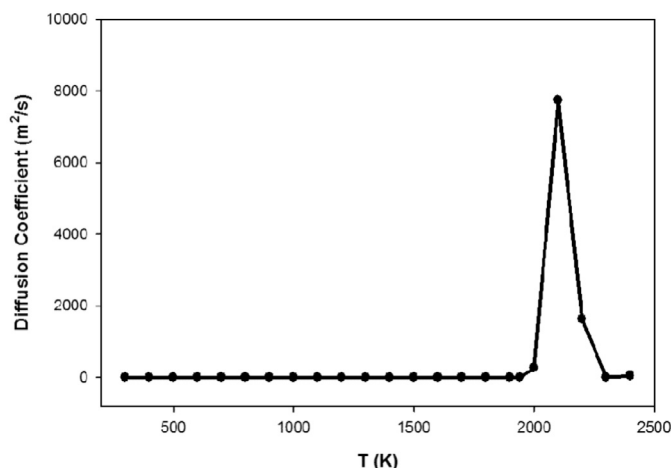
### 3.1.2. The Diffusion Coefficient for $Ti_{32}$

Figure 5 shows the diffusivity, which was calculated from the means square displacement at increasing temperature. The figure depicts no movement of atoms at temperatures lower than 1941.15 K, where the diffusivity reverts to zero. At 2000 K, the atoms appear to have a noticeable movement followed by a diffusivity jump at 2100 K, which might indicate the transition of the nanocluster from solid phase to liquid phase.

These observed transitions are justifiable since the melting temperature for Ti bulk is 1941.15 K which is closer to 2100 K. It is also noticed that as the cluster changes its shape, the diffusivity reverts to zero until the melting temperature is reached. This behaviour may be due to nanocluster transforming into a liquid phase and consequently resulting in surface melting. Similar behaviour was noted for Pd-Pt clusters.<sup>35</sup> Their transition



**Figure 4** The (a) total energy (heating and cooling) and (b) configuration energy for  $Ti_{32}$  cluster in the temperature range 300–2400 K. The melting temperature (1941.15 K) is considered to allow direct comparison of  $Ti_{32}$  nanocluster.



**Figure 5** The diffusion coefficient for the  $\text{Ti}_{32}$  cluster showing phase changes at temperatures above the bulk Ti melting.

temperature was observed to be in the temperature range 800–1200 K, corresponding to the surface melting stage.

However, both Pd and Pt diffusion coefficients tended to increase with temperature whilst a decline is observed in this study. The decline behaviour might be due to differences in atomic sizes and the number of atoms in the cluster.

### 3.1.3. Radial Distribution Function and Density Profiles for the $\text{Ti}_{32}$ Cluster

In Fig. 6a, the RDFs and the atomic distribution curves against temperature are shown. The 300 K peak shows that the nanocluster has a well-ordered structure.

However, as the temperature increases, the peaks become broader and decrease, indicating a phase change. The reduction in the probability of the peaks may be ascribed to nanocluster changing phases or fragments, which at some point will transition from a solid phase to a liquid phase at an elevated temperature near or above the melting point. This observation is in line with previous reports.<sup>41,42</sup> The reduction in the sharpness of the peaks is indicative of the reduced crystallinity of the nanocluster, which results in the production of new configurations. Thus, representing the evolution of the nanocluster during heating.

In the case of the density profile plot (Fig. 6b), the atomic distribution of  $\text{Ti}_{32}$  nanocluster along the axis at different temperatures shows various trends. At lower temperatures, the distinct

peaks indicate the solid-like features, where atoms have higher distribution at a certain distance from the centre. This plot depicts overlap of the peaks at 300 K and 800 K, suggesting that the nanocluster is still in its solid form. However, from 1400–1941.15 K, the peaks are observed to decrease and overlap, indicating minor thermally agitated changes in the system, i.e. the nanocluster is still in a solid phase.

Furthermore, it becomes easier to observe the changes along the Z (Å) axis. As the temperature increases, the peaks become broader, decreasing the peak size due to uniformly distributed atoms in the liquid phase at elevated temperatures. Moreover, at 2000 K, which is beyond the bulk melting temperature, atomic distribution becomes extensively shorter, and the new peaks emerging allude to a liquid phase formation.

## 4. Summary and Conclusion

The molecular dynamics (MD) simulations were carried out to investigate the characteristics of the ground state configuration predicted for the  $\text{Ti}_{32}$  nanocluster. The thermal agitation shows the dominance of icosahedra, and pentagonal bipyramid geometries below 2000 K. As the temperature increases, the ordering of configurations or isomers changes are noticeable by a change in the morphology of the cluster at 400 K. We also observed a jump in the potential energy at 2000 K which is closer to the melting temperature of bulk Ti suggesting a transition from a solid phase to a liquid phase. The maxima in the potential energy occur at a temperature above bulk melting. However, upon cooling, the nanocluster is mostly solid below the melting temperature. We notice a weak hysteresis at 2000 K due to the structural changes as we cool the temperature.

As a consequence, the cooling transition occurs close to the melting temperature with the nanocluster, which is equivalent to the initial one. The diffusion coefficient results suggest no movement of atoms at temperatures below 1941.15 K; thus, the diffusivity reverts to zero. A noticeable vibration is observed above 2000 K, resulting in a jump in diffusivity at 2100 K. The RDFs shows the peaks decreasing with increasing temperature, and the density profiles reveal the melting temperature behaviour beyond bulk melting temperature, where atomic distribution becomes broader and shorter, and the new peaks emerging.

## Acknowledgements

The work was carried out at the Materials Modelling Centre,

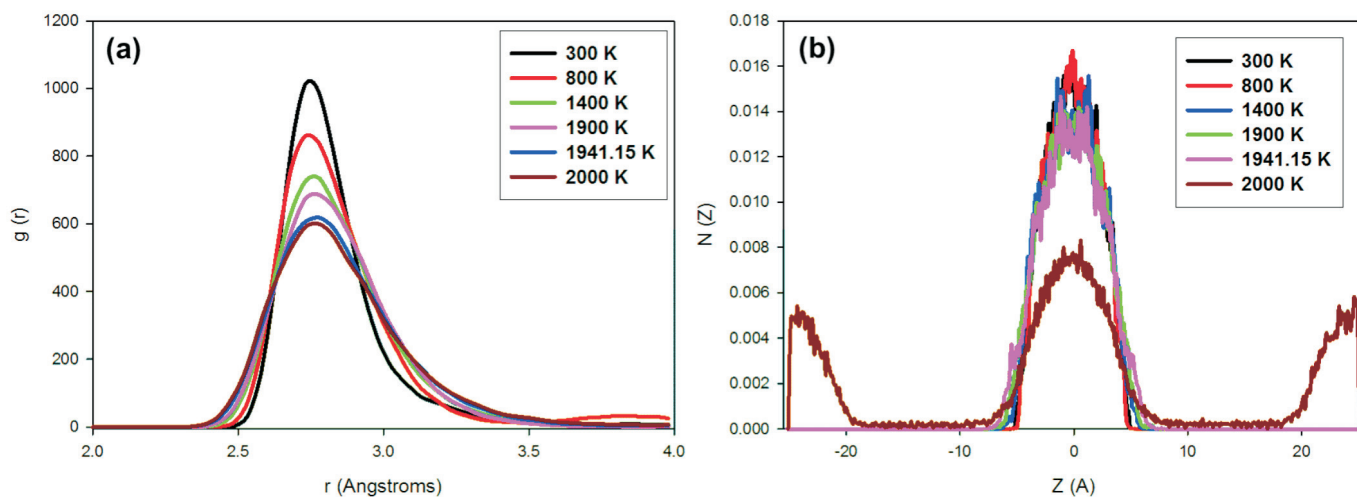


**Figure 6** (a) Radial distribution functions (RDF) and (b) the atomic distribution of  $\text{Ti}_{32}$  nanocluster along a Cartesian coordinate ( $z$ ) at different temperatures.

the University of Limpopo, in collaboration with the University College London, the UCL Faraday high performance computing and the Centre for High-Performance Computing (CHPC) in South Africa. We also acknowledge the support from the South African Research Chair Initiative of the Department of Science and Technology, the National Research Foundation and the Royal Society Advanced Fellowship Newton Grant (NA140447).

### Supplementary Material

Supplementary information is provided in the online supplement.

### ORCID iDs

T.M. Phaahla:  [orcid.org/0000-0002-0878-2532](https://orcid.org/0000-0002-0878-2532)  
A.A. Sokol:  [orcid.org/0000-0003-0178-1147](https://orcid.org/0000-0003-0178-1147)  
C.R.A. Catlow:  [orcid.org/0000-0002-1341-1541](https://orcid.org/0000-0002-1341-1541)  
S.M. Woodley:  [orcid.org/0000-0003-3418-9043](https://orcid.org/0000-0003-3418-9043)  
P.E. Ngoepe:  [orcid.org/0000-0003-0523-5602](https://orcid.org/0000-0003-0523-5602)  
H.R. Chauke:  [orcid.org/0000-0003-2603-5941](https://orcid.org/0000-0003-2603-5941)

### References

- J.D. Aiken III, Y. Lin, R.G. Finke and J. Mol, A perspective on nanocluster catalysis: polyoxoanion and  $(n-C_4H_9)_4N^+$  stabilized  $Ir(0)\sim 300$  nanocluster 'soluble heterogeneous catalysts', *J. Mol. Catal. A: Chem.*, 1996, **114**, 29–51.
- U. Simon, G. Schon and G. Schmid, The application of  $Au^{55}$  clusters as quantum dots, *Angew. Chem. Int. Ed. Engl.*, 1993, **32**, 250–254.
- V.L. Colvin, M.C. Schlamp and A.P. Alivisatos, Light-emitting diodes made from cadmium selenide nanocrystals and a semiconducting polymer, *Nature*, 1994, **370**, 354.
- R. Pool, Clusters: Strange morsels of matter: when metals or semiconductors are shrunk down to clumps only 10 or 100 atoms in size, they become a "totally new class of materials" with potentially valuable applications, *Science*, 1990, **248**, 1186.
- M. Schmidt, R. Kusche, W. Kronmuller, B. Von Issendorff and H. Haberland, experimental determination of the melting point and heat capacity for a free cluster of 139 sodium atoms, *Phys. Rev. Lett.*, 1997, **79**, 99.
- F. Ercolessi, W. Andreoni and E. Tosatti, Melting of small gold particles: mechanism and size effects, *Phys. Rev. Lett.*, 1991, **66**, 911.
- M. Schmidt, K. Kusche, B.V. Issendorff and H. Haberland, Irregular variations in the melting point of size-selected atomic clusters, *Nature*, 1998, **393**, 238.
- K.F. Peters, J.B. Cohen and Y.-W. Chung, Melting of Pb nanocrystals, *Phys. Rev. B*, 1998, **57** 13430.
- R.R. Couchman, The Lindemann hypothesis and the size dependence of melting temperatures. II, *Philos. Mag. A*, 1979, **40**, 637.
- S.C. Hendy and B.D. Hall, Molecular-dynamics simulations of lead clusters, *Phys. Rev. B*, 2001, **64**, 085425.
- P. Labastie and R.L. Whetten, Statistical thermodynamics of the cluster solid-liquid transition, *Phys. Rev. Lett.*, 1990, **65**, 1567.
- F. Calvo and R. Spiegelman, Mechanisms of phase transitions in sodium clusters: From molecular to bulk behavior, *J. Chem. Phys.*, 2000, **112**, 2888.
- J.Y. Lee, E.K. Lee and R.M. Nieminen, Effect of potential energy distribution on the melting of clusters, *Phys. Rev. Lett.*, 2001, **86**, 999.
- D.J. Wales and R.S. Berry, Freezing, melting, spinodals, and clusters, *J. Chem. Phys.*, 1990, **92**, 4473.
- M. Schmidt, J. Donges, Th. Hippler and H. Haberland, Influence of energy and entropy on the melting of sodium clusters, *Phys. Rev. Lett.*, 2003, **90**, 103401.
- M. Schmidt and H. Haberland, Phase transitions in clusters, *C. R. Physique*, 2002, **3**, 327.
- Y.G. Chushak and L.S. Bartell, Melting and freezing of gold nanoclusters, *J. Phys. Chem. B*, 2001, **105**, 11605.
- B. Wang, G. Wang, X. Chen and J. Zhao, Melting behavior of ultrathin titanium nanowires, *Phys. Rev. B*, 2003, **67**, 193403.
- C.L. Cleveland, W.D. Luedtke and U. Landman, Melting of gold clusters, *Phys. Rev. B*, 1999, **60**, 5065–5077.
- J.P. Borel, Thermodynamical size effect and the structure of metallic clusters, *Surf. Sci.*, 1981, **106**, 1.
- J. Bovin, R. Wallenbreg and D. Smith, Imaging of atomic clouds outside the surfaces of gold crystals by electron microscopy, *Nature*, 1985, **47**, 317.
- J. Luo, U. Landman and J. Jortner, 1987, *Physics and Chemistry of Small Clusters* (P. Jena, B.K. Rao and S.N. Khanna, eds.), Plenum, New York, USA, p. 201.
- T.P. Martin, Alkali halide clusters and microcrystals, *J. Phys. Rep.*, 1983, **95**, 167.
- G. Breaux, D. Hillman, C. Neal, R. Benirschke and M. Jarrold, Gallium Cluster "Magic Melters", *J. Am. Chem. Soc.*, 2004, **126**, 8628.
- G. Breaux, B. Cao and M.F. Jarrold, Second-order phase transitions in amorphous gallium clusters, *J. Phys. Chem. B*, 2005, **109**, 16575.
- T. Lazauskas, A.A. Sokol, J. Buckeridge, C.R.A. Catlow, S.G.E.T. Escher, M.R. Farrow, D. Mora-Fonz, V.W. Blum, T.M. Phaahla, H.R. Chauke, P.E. Ngoepe and S.M. Woodley, Thermodynamically accessible titanium clusters  $Ti_N$ ,  $N = 2\text{--}32$ , *Phys. Chem. Chem. Phys.*, 2018, **20**, 13962–13973.
- S.M. Woodley, Knowledge Led master code search for atomic and electronic structures of  $LaF_3$  nanoclusters on hybrid rigid ion–shell model–DFT landscapes, *J. Phys. Chem. C*, 2013, **117**, 24003–24014.
- J.D. Gale and A.L. Rohl, The General Utility Lattice Program (GULP), *Mol. Simul.*, 2003, **29**, 291–341.
- V. Blum, R. Gehrke, F. Hanke, P. Havu, V. Havu, X. Ren, K. Reuter and M. Scheffler, Ab initio molecular simulations with numeric atom-centered orbitals, *Comp. Phys.*, 2009, **180**, 2175–2196.
- R.P. Gupta, Lattice relaxation at a metal surface, *Phys. Rev. B*, 1981, **23**, 6265.
- F. Cleri and V. Rosato, Tight-binding potentials for transition metals and alloys, *Phys. Rev. B*, 1993, **48**, 22.
- D. Tomanek, A.A. Aligia and C.A. Balseiro, Calculation of elastic strain and electronic effects on surface segregation, *Phys. Rev. B*, 1985, **32**, 5051.
- Official DL\_POLY\_4 website at: [https://www.scd.stfc.ac.uk/Pages/DL\\_POLY.aspx](https://www.scd.stfc.ac.uk/Pages/DL_POLY.aspx)
- W. Hoover, Canonical dynamics: equilibrium phase-space distributions, *Phys. Rev. A*, 1985, **31**, 1695–1697.
- S.K.R.S. Sankaranarayanan, V.R. Bhethanabotla and J. Babu, Molecular dynamics simulation study of the melting of Pd-Pt nanoclusters, *Phys. Rev. B*, 2005, **71**, 195415.
- M.C. Steele and R.A. Hein, Superconductivity of titanium, *Phys. Rev.*, 1953, **92**, 243–247.
- C. Kittel, 2004, *Introduction to Solid State Physics*, 8th edn., John Wiley & Sons, New York, USA.
- Y. Qi, T. Çağın, W.L. Johnson and W.A. Goddard, Melting and crystallization in Ni nanoclusters: the mesoscale regime, *J. Chem. Phys.*, 2001, **115**, 385.
- C. Majumder, V. Kumar, H. Mizuseki and Y. Kawazoe, Small clusters of tin: atomic structures, energetics, and fragmentation behavior, *Phys. Rev. B*, 2001, **64**, 233405.
- K. Joshi, D.G. Kanhere and S.A. Blundell, Abnormally high melting temperature of the  $Sn_{10}$  cluster, *Phys. Rev. B*, 2002, **66**, 155329.
- A.S. Barnard, Modelling of nanoparticles: approaches to morphology and evolution, *J. Rep. Prog. Phys.*, 2010, **73**, 086502.
- S.L. Gafner, L.V. Redel and Y.Y. Gafner, Simulation of the processes of structuring of copper nanoclusters in terms of the tight-binding potential *J. Exp. Theor.*, 2009, **108**, 784–799.

### **Supplementary material to:**

T.M. Phaahla, A.A. Sokol, C.R.A. Catlow, S.M. Woodley, P.E. Ngoepe and H.R. Chauke,

The Thermal Agitated Phase Transitions on the  $Ti_{32}$  Nanocluster: a Molecular Dynamics Simulation Study,

*S. Afr. J. Chem.*, 2021, **74** (Special Edition), 17–22.

## Supplementary information, S. Afr. J. Chem.

### The thermal agitated phase transitions on the Ti<sub>32</sub> nanocluster: A molecular dynamics simulation study

Tshegofatso M. Phaahla<sup>1</sup>, Alexey A. Sokol<sup>2</sup>, Charles R. A. Catlow<sup>2,1</sup>, Scott M. Woodley<sup>2</sup>, Phuti E. Ngoepe<sup>1</sup>, and Hasani R. Chauke<sup>1</sup>

<sup>1</sup> *Materials Modelling Centre, University of Limpopo, Private Bag x1106, Sovenga 0727, South Africa.*

<sup>2</sup> *University College London, Kathleen Lonsdale Materials Chemistry, Department of Chemistry, 20 Gordon Street, London WC1H 0AJ, United Kingdom*

*E-mail: Corresponding.hasani.chauke@ul.ac.za*

#### TABLE OF CONTENTS

1. Lattice geometry and ionic positions for Ti<sub>32</sub> at 300 K.
2. Lattice geometry and ionic positions for Ti<sub>32</sub> at 400 K.
3. Lattice geometry and ionic positions for Ti<sub>32</sub> at 500 K.
4. Lattice geometry and ionic positions for Ti<sub>32</sub> at 600 K.
5. Lattice geometry and ionic positions for Ti<sub>32</sub> at 700 K.
6. Lattice geometry and ionic positions for Ti<sub>32</sub> at 800 K.
7. Lattice geometry and ionic positions for Ti<sub>32</sub> at 900 K.
8. Lattice geometry and ionic positions for Ti<sub>32</sub> at 1000 K.
9. Lattice geometry and ionic positions for Ti<sub>32</sub> at 1100 K.
10. Lattice geometry and ionic positions for Ti<sub>32</sub> at 1200 K.
11. Lattice geometry and ionic positions for Ti<sub>32</sub> at 1300 K.
12. Lattice geometry and ionic positions for Ti<sub>32</sub> at 1400 K.
13. Lattice geometry and ionic positions for Ti<sub>32</sub> at 1500 K.
14. Lattice geometry and ionic positions for Ti<sub>32</sub> at 1600 K.
15. Lattice geometry and ionic positions for Ti<sub>32</sub> at 1700 K.
16. Lattice geometry and ionic positions for Ti<sub>32</sub> at 1800 K.
17. Lattice geometry and ionic positions for Ti<sub>32</sub> at 1900 K.
18. Lattice geometry and ionic positions for Ti<sub>32</sub> at 1941.15 K.
19. Lattice geometry and ionic positions for Ti<sub>32</sub> at 2000 K.
20. Lattice geometry and ionic positions for Ti<sub>32</sub> at 2100 K.
21. Lattice geometry and ionic positions for Ti<sub>32</sub> at 2200 K.
22. Lattice geometry and ionic positions for Ti<sub>32</sub> at 2300 K.
23. Lattice geometry and ionic positions for Ti<sub>32</sub> at 2400 K.



1. Lattice geometry and ionic positions for Ti<sub>32</sub> at 300 K.

Format: XYZ file

```
50.0000000000    0.0000000000    0.0000000000
0.0000000000    50.0000000000    0.0000000000
0.0000000000    0.0000000000    50.0000000000

Ti -4.54666545   1.74008362   1.49626329
Ti -4.74260780   0.83178665  -0.94363262
Ti -3.93857361   3.56455838  -0.77847782
Ti -3.44661830  -0.58587495   0.96884685
Ti -2.86438705   3.64574343   1.97224577
Ti -1.86628293   1.17602400   2.45751194
Ti -1.45731630   4.82527912  -0.07961654
Ti -2.22244554   1.73076495  -0.13462636
Ti -3.29633106   1.66934408  -2.96571585
Ti -2.70980713  -0.88948005  -1.64899221
Ti -1.56272073   3.48356872  -2.40635320
Ti -0.18918204   3.31514708   2.01151072
Ti -0.79635752  -0.62136586   0.24574287
Ti  1.23391571   5.14361754   0.55237043
Ti  0.34551076   2.76665599  -0.55571768
Ti -0.96920349   1.91855838  -4.65449581
Ti  0.47842810   5.20014434  -1.97460115
Ti -0.66291296   0.83355581  -2.20900978
Ti  0.80102965   0.79761610   1.58925932
Ti -1.78031608  -0.57955159  -4.12812922
Ti -0.01979110  -1.72291643  -2.09862714
Ti  1.19405491   2.60081483  -3.06891562
Ti  2.52784968   2.88427990   1.35294614
Ti  1.70964301  -1.77567569   0.17361538
Ti  1.85758286   0.58270254  -0.93360122
Ti  2.87137486   3.73030728  -1.34210858
Ti  1.18976486   0.10448976  -3.97688516
Ti  2.64850135  -1.60545951  -2.48913107
Ti  3.39159575   0.08627286   1.47896064
Ti  3.62493641   1.13163737  -2.86948315
Ti  4.47836651   1.84410858  -0.27256971
Ti  4.38206540  -0.75346386  -0.72460533
```

## 2. Lattice geometry and ionic positions for Ti<sub>32</sub> at 400 K.

Format: XYZ file

```
50.0000000000    0.0000000000    0.0000000000
0.0000000000    50.0000000000    0.0000000000
0.0000000000    0.0000000000    50.0000000000

Ti -4.15034675   0.81071942   1.07919770
Ti -1.66498732   0.72058195   2.92653810
Ti -2.45450665  -1.68340147   2.22278357
Ti -3.16925349   2.76521789  -0.61044415
Ti -3.61481680  -1.63718299  -0.18759115
Ti -3.97418679   0.51697644  -1.79343332
Ti -0.88507568  -2.34006679  -0.12833933
Ti -1.67664904   0.35608167   0.15071520
Ti -2.28010480   2.99242155   1.88612808
Ti -2.00267641   5.17635460   0.09484103
Ti  0.34958697  -0.91309648   1.80015064
Ti -1.93118552  -1.10138853  -2.29917785
Ti -1.38178230   4.23215078  -2.43663289
Ti  0.79077896  -1.67053897  -2.40469297
Ti  0.83650568   0.40394662  -0.77167824
Ti  0.65827303   1.69156423   2.03394484
Ti  1.86980041  -2.21002146  -0.00447775
Ti -0.56320497   2.83184160  -0.15752934
Ti -1.25735267   1.40461851  -2.32974064
Ti  0.02512697   4.60266125   1.76664904
Ti  0.62213888   5.28989713  -0.73034548
Ti  2.92963720   0.43077655   0.90637029
Ti -0.42254849  -0.02188247  -4.40477325
Ti  0.95352590   5.30016120  -3.48396169
Ti  1.19677610   3.03773620  -2.09487277
Ti  3.38094235  -0.71642148  -1.76874337
Ti  2.26385327   3.25908085   0.46697717
Ti  3.23544667   4.71321769  -1.85844637
Ti -0.16794330   2.70319041  -4.52609440
Ti  3.55638698   1.94293068  -1.59635121
Ti  1.86191522   0.82195192  -3.47368339
Ti  2.72902711   3.36319485  -4.22930796
```

### 3. Lattice geometry and ionic positions for Ti<sub>32</sub> at 500 K.

Format: XYZ file

```
50.0000000000    0.0000000000    0.0000000000
0.0000000000    50.0000000000    0.0000000000
0.0000000000    0.0000000000    50.0000000000

Ti    0.431972 -0.224854 -3.542267
Ti    2.897534 -1.520845 -2.343975
Ti    2.658995  1.249110 -3.112118
Ti    0.226155 -2.493015 -2.013282
Ti    0.655416  2.207507 -4.868825
Ti   -1.980367  1.361883 -3.933204
Ti    4.297407  0.732940 -1.027029
Ti    1.357897 -0.084555 -0.795566
Ti    3.550624 -1.163240  0.602470
Ti    1.742918 -2.930926  0.066339
Ti    2.783841  1.335689  1.312494
Ti   -0.983798  4.100081 -3.633721
Ti   -1.477891  0.210078 -1.208908
Ti    1.858316  4.003276 -3.230742
Ti    0.268102  2.104423 -2.213450
Ti    0.944222  1.644117  3.196959
Ti    2.545788  2.872452 -0.766102
Ti   -0.026863  1.830855  0.530783
Ti   -3.686531  3.581806 -3.216739
Ti    1.134331 -0.772075  1.864785
Ti   -0.765159 -1.877976  0.433411
Ti    0.993396  3.983696  1.632397
Ti   -2.501292  5.505766 -1.813020
Ti   -4.109502  1.346860 -1.678718
Ti   -2.021363  2.889233 -1.408389
Ti    0.256397  4.624318 -1.110152
Ti   -1.358791  0.224656  2.236267
Ti   -3.377079 -0.774116  0.318341
Ti   -4.390863  3.832885 -0.657041
Ti   -1.406292  2.861327  2.785219
Ti   -1.820761  4.519904  0.820869
Ti   -3.033658  1.892015  0.816893
```

4. Lattice geometry and ionic positions for  $\text{Ti}_{32}$  at 600 K.

Format: XYZ file

```
50.0000000000    0.0000000000    0.0000000000
0.0000000000    50.0000000000    0.0000000000
0.0000000000    0.0000000000    50.0000000000

Ti  4.29359883  1.41865620 -2.44312250
Ti  4.25121065 -0.11030434 -0.21956876
Ti  3.23051587  2.56783029  0.09783292
Ti  3.32596181 -1.21450902 -2.70886218
Ti  2.25411930  3.23122101 -2.58424074
Ti  2.06023180  0.92910484 -4.15700882
Ti  2.23913248  5.00285209 -0.56937434
Ti  1.93729541  0.75032928 -1.44484538
Ti  1.95515088  0.56996537  1.40502599
Ti  2.07215402 -1.78170234 -0.13497883
Ti  1.26716669  3.37942879  2.04186801
Ti  0.34490949  3.17257792 -4.43047323
Ti  0.58473629 -1.39753514 -2.66585423
Ti -0.05253500  4.91451513 -2.08628202
Ti  0.36587451  2.77837526 -0.38478443
Ti -0.65138587  1.04470602  1.91664676
Ti -0.13385767  5.59165962  0.58398321
Ti -0.11506535 -0.15920164 -0.28211572
Ti -0.39679602  1.33649691 -2.67071054
Ti  0.11896375 -1.71340798  1.92969935
Ti -0.58409531 -2.78214534 -0.39017163
Ti -1.61182069  3.53770840  1.78850290
Ti -2.00457520  3.44850494 -3.09735809
Ti -2.25097746 -1.08551531 -1.92162247
Ti -2.08857228  1.72666164 -0.54548517
Ti -2.39332938  4.45752146 -0.70682576
Ti -3.26463352  1.11225781  1.99551349
Ti -2.43689156 -1.16166572  0.86548435
Ti -3.30636616  1.01332173 -3.13614690
Ti -4.39204480  3.06181250  0.59126314
Ti -4.54774613  2.99201908 -1.98757706
Ti -4.40722865  0.44173393 -0.60443321
```

5. Lattice geometry and ionic positions for  $\text{Ti}_{32}$  at 700 K.

Format: XYZ file

```
50.0000000000    0.0000000000    0.0000000000
0.0000000000    50.0000000000    0.0000000000
0.0000000000    0.0000000000    50.0000000000

Ti  2.94256387  1.64989933  1.43067445
Ti  1.99100525 -0.80108794  2.50990522
Ti  1.13739957  4.22237711  1.65562647
Ti  1.27351528 -2.67696880  0.65991985
Ti  3.49051221  3.65609936 -0.27777744
Ti  1.84843300 -1.44242403 -2.00344207
Ti  3.54863679 -1.10329939  0.34483776
Ti  1.15596676  0.02147128  0.19003386
Ti  0.29660268  1.47842336  2.35024399
Ti -0.65753648 -1.15206630  1.86221756
Ti  0.81393962  2.79464934 -0.42054729
Ti  2.39183002  0.41720303 -3.80025914
Ti -0.68025708 -1.66139698 -1.10902421
Ti  3.11286234  1.08862291 -1.23254045
Ti  0.13866430  0.97291539 -2.32230677
Ti -2.62644125  0.73234310  2.45175281
Ti  1.62811720  5.25752493 -1.18024726
Ti -1.34002912  0.76561992  0.12152141
Ti -0.23311436 -0.94957804 -4.06145482
Ti -3.14811501 -1.11818834  0.37588329
Ti -2.68239931  0.05171042 -2.34133097
Ti -1.69792149  3.15089396  1.34274860
Ti  2.20605423  2.98359309 -2.91684122
Ti -1.97875015  1.95530405 -4.08713711
Ti -1.84074687  2.73253805 -1.38849236
Ti -0.93012841  5.13040268 -0.49663162
Ti -3.96184430  1.53726770  0.12351731
Ti -4.36482209  2.38093427 -2.50149547
Ti -0.10348232  4.09118343 -3.09008667
Ti -3.69808332  4.25213183 -0.27530976
Ti -2.80397515  4.68185459 -3.02578447
Ti  0.43464433  1.97332006 -4.84419536
```

6. Lattice geometry and ionic positions for  $\text{Ti}_{32}$  at 800 K.

Format: XYZ file

```
50.0000000000    0.0000000000    0.0000000000
0.0000000000    50.0000000000    0.0000000000
0.0000000000    0.0000000000    50.0000000000

Ti -0.52136975 -2.93398761 -1.34305914
Ti -1.62217820 -1.15158052 -3.03788326
Ti  0.03637871 -0.56328421 -0.08950942
Ti  1.28103170 -1.18327619 -2.24720958
Ti -2.50878749 -0.92734153 -0.46435149
Ti  1.70403779 -2.57576437  0.22551719
Ti -0.93482801 -2.79235319  1.31224332
Ti -0.50066413  1.00204248 -2.19697235
Ti -1.92657528  1.25404474 -4.55023118
Ti  0.56656198  0.13733766 -4.54868979
Ti -4.09669857  0.97238275  0.83880664
Ti  2.99784873  1.76436881  1.89163210
Ti  2.47499938  1.33086999 -2.68809948
Ti  1.66983131 -0.63472883  2.01952919
Ti  1.30546897  1.66252941 -0.16221594
Ti -3.05255496  1.26194614 -2.10072389
Ti -2.43222944  2.39201102  2.29702410
Ti -0.11551544  3.51635791 -1.37697404
Ti  3.16410079 -0.22357860 -0.24889119
Ti -2.32739921  3.67524186 -2.84797828
Ti  0.28146894  2.71426904 -4.04986375
Ti -3.38372905  3.57618380 -0.17688177
Ti  0.29190906  1.63228662  2.33244983
Ti  2.25022506  3.98218979 -2.40401393
Ti -1.52400583  1.71508347  0.04040262
Ti -1.67769808 -0.22224897  2.04212585
Ti -1.89994532  5.70940292 -1.24485561
Ti -0.12040828  5.25267707 -3.33916893
Ti  3.89635511  2.47964237 -0.59949246
Ti -0.63811076  4.25537321  1.07523937
Ti  2.11516016  4.08209773  0.62009789
Ti  0.91042085  5.91307861 -0.93402448
```

7. Lattice geometry and ionic positions for  $\text{Ti}_{32}$  at 900 K.

Format: XYZ file

```
50.0000000000    0.0000000000    0.0000000000
0.0000000000    50.0000000000    0.0000000000
0.0000000000    0.0000000000    50.0000000000

Ti -3.22996327  0.60239816 -1.40296004
Ti -1.04883704  4.20218064  0.68227035
Ti -1.84030362  0.48660635 -3.64266440
Ti  1.63142563  3.93566179  1.83143631
Ti -3.28606210  2.80719242 -3.12233180
Ti -3.48210412  3.30667391 -0.53368342
Ti  0.15639020 -1.87514308 -3.42661313
Ti -1.99012339  1.53539678  0.69403349
Ti -3.26001328  3.15090480  2.39254881
Ti -0.51051023  2.19884396  2.88105484
Ti -4.56727418  0.80953351  1.21428263
Ti -1.04379139  2.99134215 -4.51765070
Ti  0.75037985  1.94445231  0.36687243
Ti  0.00118490 -2.39364355 -0.27401413
Ti -0.38556957 -0.04690457 -1.32015894
Ti -2.60916537  0.48172604  3.12404671
Ti -2.05978383 -1.89461569 -1.93876591
Ti  2.04885609  1.60303943 -1.75046146
Ti -1.41452278  4.88010930 -2.22556448
Ti  2.16179901  1.25318001  2.58230814
Ti  3.48075161  2.51507952  0.41467994
Ti -2.38980031 -1.09498221  0.68996465
Ti  0.70432320  0.79305477 -3.97020842
Ti  1.19872725  4.34400053 -0.93448605
Ti -0.86495946  2.42719587 -1.73624700
Ti  2.17727724 -0.38756730  0.08264209
Ti -0.11743893 -0.28998539  1.75966624
Ti  4.62302582  0.91900711 -1.65037781
Ti  1.24338778  3.46228236 -3.54309950
Ti  2.51459856 -0.79026951 -2.51250685
Ti  3.28686672  1.47828883 -4.00002807
Ti  3.78432974  3.71823415 -2.17000639
```

8. Lattice geometry and ionic positions for  $\text{Ti}_{32}$  at 1000 K.

Format: XYZ file

```
50.0000000000    0.0000000000    0.0000000000
0.0000000000    50.0000000000    0.0000000000
0.0000000000    0.0000000000    50.0000000000

Ti  0.71983952  1.54236427 -4.33744936
Ti  3.04082485 -0.43410389 -1.05150172
Ti  1.12219514 -2.46730775 -0.24143506
Ti  2.57989018  3.31090161 -4.01335977
Ti -1.60442292  2.86940159 -4.59238115
Ti -0.01976401  5.44788204 -0.68691106
Ti  0.74507634  1.00711282  2.20329608
Ti  1.70955732  1.78555077 -1.97491140
Ti -0.97653286 -1.91871064 -1.90814120
Ti -3.58784265  2.80126782  2.27453060
Ti  0.97876500 -0.78357510 -2.96088287
Ti  4.26007668  2.24465001 -1.99362096
Ti -1.48213106  0.24785127 -3.56006427
Ti  0.45548462 -0.04312178 -0.38084233
Ti -3.39271051  2.05353022 -3.05803191
Ti -3.91697168  0.18980307  1.40606071
Ti  3.26951151  0.53150142 -3.76520628
Ti -1.65986930  1.44648807  0.79057499
Ti  2.56149189  4.24092203 -1.23596715
Ti  0.42878918 -1.73735168  2.28911122
Ti -1.85952457  0.28482548  3.06704141
Ti -1.63741926 -1.22923504  0.69958493
Ti  3.18339835  1.92435005  0.42280213
Ti -3.75911370  2.66044463 -0.57926630
Ti -0.91689248  2.29807767 -1.78320148
Ti  0.39439738  4.50847049 -3.16355104
Ti -0.96601102  3.02977444  2.93389238
Ti -2.29782611  4.63884834 -2.28708503
Ti -3.10366386  0.02645222 -1.10219431
Ti -2.05289735  4.24546053  0.66485012
Ti  0.74911502  3.11696319  0.44206530
Ti  2.69828111 -0.76621482  1.52617291
```



9. Lattice geometry and ionic positions for  $\text{Ti}_{32}$  at 1100 K.

Format: XYZ file

```
50.0000000000    0.0000000000    0.0000000000
0.0000000000    50.0000000000    0.0000000000
0.0000000000    0.0000000000    50.0000000000

Ti -1.10116610  2.51277279 -3.09873473
Ti -0.71768472 -0.06902173 -3.14657944
Ti -2.75171575 -0.91827436 -1.09506641
Ti  1.35340181  1.32677274 -4.20827225
Ti  3.54822441  3.32229705 -4.55566754
Ti -1.07901968  0.89299191  3.68701495
Ti  3.58704658  1.50692572 -1.99954380
Ti -2.73663077  3.62179580 -1.23758972
Ti -3.43600701  1.21683142 -2.57894897
Ti -2.04115954  2.64850008  1.53282095
Ti -1.42536518 -2.67411746  1.04170785
Ti -0.66635778  5.10925197 -2.75206240
Ti -4.23438170  1.24115361  0.07928708
Ti  2.67789668  3.24414445 -0.08857145
Ti  1.61494237  3.60038252 -2.59660965
Ti -2.24930555 -1.45080805  3.60741074
Ti  0.03981925 -0.89450330 -0.65701925
Ti -4.00322185  0.85133094  2.77664902
Ti -2.04289442 -0.05804546  1.28410017
Ti  2.04483285 -2.47479569  0.40448154
Ti  1.82346792  5.75245436 -1.03079216
Ti  0.48859664  1.44358002  1.48230585
Ti  2.06513443 -0.86243721 -2.37753511
Ti -0.16666897  3.75639200 -0.42957167
Ti  1.00255808  1.48316247 -1.41603751
Ti  2.12052925  5.73668983 -3.94765070
Ti -4.13293113 -1.53165196  1.29047307
Ti  2.54824756  0.19034793  0.16611722
Ti  4.08558071  4.64983554 -2.28884249
Ti  0.33044392 -1.26092030  2.17262547
Ti -1.54373405  1.33626205 -0.82816981
Ti  0.66062250  3.82397369 -5.14775071
```

10. Lattice geometry and ionic positions for  $\text{Ti}_{32}$  at 1200 K.

Format: XYZ file

```
50.0000000000    0.0000000000    0.0000000000
0.0000000000    50.0000000000    0.0000000000
0.0000000000    0.0000000000    50.0000000000

Ti -3.24994521 -2.29358213  0.18457825
Ti -0.07733300  4.30548945 -3.40084304
Ti -1.32328876  2.05756170  1.73866155
Ti -0.72899120  0.80254119 -1.87506096
Ti  0.75059424  1.34458696  0.22127903
Ti -1.18996287 -1.77154529 -1.94420488
Ti -2.41889544  2.44336569 -3.37010598
Ti  3.79253372  0.87152226 -3.60060572
Ti -4.19504149  0.18364144  0.94903729
Ti -2.69833438 -1.35595344  2.64519023
Ti -0.60339485  3.29565492 -0.96397467
Ti -1.45516907 -0.15145359 -4.17916099
Ti  2.64879154  3.56721322 -3.99337839
Ti  3.17556464  0.11421514 -1.04233542
Ti -2.31562991  4.52187230  0.91797809
Ti  1.30129129 -0.46286039 -3.22026086
Ti -2.98436291  2.26670182 -0.43739274
Ti -1.65302524 -0.20353860  0.38538538
Ti  0.32140246  4.33926089  1.20665127
Ti -0.62801968 -2.81786109  1.28740325
Ti  1.75477273  4.60130562 -1.30801220
Ti -3.38855983  0.18031895 -1.86976740
Ti  1.65224765  2.08968402 -2.17749931
Ti -0.67513007  5.90648495 -0.89349989
Ti  2.70268603  0.11443077  1.62094006
Ti  1.38611890  2.31261115  2.74287463
Ti  0.08879315 -0.33751845  2.43426578
Ti  0.95119183 -1.29325621 -0.38517678
Ti  0.54034805  1.87482876 -4.47165403
Ti -2.80304919  4.79755528 -1.82183287
Ti  2.88540303  2.78869267  0.49152020
Ti  4.09949457  2.98130343 -1.82702076
```

11. Lattice geometry and ionic positions for  $\text{Ti}_{32}$  at 1300 K.

Format: XYZ file

```
50.0000000000    0.0000000000    0.0000000000
0.0000000000    50.0000000000    0.0000000000
0.0000000000    0.0000000000    50.0000000000

Ti -2.14023985  2.35584763 -3.16680627
Ti  1.42132756 -0.60227100  1.53601269
Ti -2.94429809 -2.30919996  0.99966712
Ti -2.39214659  1.56865126  3.74201568
Ti -0.57721432 -0.96212111 -0.17328831
Ti -4.01279510  2.12691615 -0.69527723
Ti  1.05363918  1.39807770 -0.42276145
Ti -5.04694538 -0.36687692  0.48961219
Ti  2.69431733  3.74616808 -1.05711377
Ti -4.58104829  1.70081752  2.27413665
Ti -0.17889041  0.51127668 -2.75788683
Ti  2.08716807 -0.82900202 -1.58209540
Ti -2.80997609 -0.11008548 -1.73499433
Ti  0.31734266  3.33716690 -2.24055346
Ti -1.38486355  2.09956798 -0.65266394
Ti  0.59091760  2.36830974 -4.86889379
Ti  0.07274551  1.45912254  2.15263610
Ti -3.77868975 -0.88424633  3.06867354
Ti -1.99454242  4.57400742 -1.51709890
Ti  2.47121438  2.68502166  1.69399889
Ti  4.43936799  0.07826240 -3.06296060
Ti -0.74816154  4.61863866 -4.10247913
Ti  4.71786262  2.58959858 -2.70162117
Ti  2.35075410  1.62506415 -2.93309854
Ti  3.58098495  2.30750835 -5.22153180
Ti  1.93800104 -0.42817406 -4.65389219
Ti  3.82740011  1.23525397 -0.45358763
Ti  0.18683103  3.88626630  0.45535281
Ti -2.23323927  3.26421770  1.85672834
Ti -2.49009812  0.56584639  1.09616741
Ti -1.05298897 -0.96332773  2.73554369
Ti  2.27936433  4.42697025 -4.05796225
```

12. Lattice geometry and ionic positions for Ti<sub>32</sub> at 1400 K.

Format: XYZ file

```
50.0000000000    0.0000000000    0.0000000000
0.0000000000    50.0000000000    0.0000000000
0.0000000000    0.0000000000    50.0000000000

Ti  2.04567109  4.62404136 -3.15556015
Ti -2.40844808  3.29059112  2.08218676
Ti  2.09245054 -0.19806638 -3.42484706
Ti  2.10071023 -0.60853241 -0.83537513
Ti  3.48389637  1.41570666  0.36648480
Ti -0.29029794  3.99438662  0.99568104
Ti -0.72897762 -0.59267823  0.11965627
Ti  4.34674700  0.50361935 -2.23880683
Ti -0.03637733 -1.70052218 -2.39049032
Ti -2.12340792  1.81217523 -0.02549767
Ti  3.59602071  2.56851869 -4.19208774
Ti -1.48249586  0.57998585  2.43675874
Ti -3.33479074 -0.88521241  0.91311690
Ti  2.10891804  4.21256991 -0.09146371
Ti -2.53665409  2.46309045 -2.59487170
Ti  0.85259401 -2.83232676  0.15706875
Ti -0.06880155  3.42120501 -1.64550189
Ti  0.40910331  5.96735000 -1.35169931
Ti  1.18908076 -0.80305628  1.92616220
Ti  0.85333906  2.46589692 -4.25285244
Ti -1.25622731 -2.36452617  1.99391252
Ti -4.37916909  3.41471410 -0.11663065
Ti -2.51240571 -0.60174441 -1.92219830
Ti -0.02027526  0.82694033 -1.92898266
Ti -1.16253269  4.74592676 -3.59169569
Ti -4.64602356  0.91323883 -0.73321852
Ti  2.21469557  2.14363092 -1.91000775
Ti  4.55212176  3.33067882 -1.83494234
Ti -2.10914616  4.94203233 -0.69212737
Ti -1.82964299 -2.89699972 -0.66564214
Ti -4.14683293  1.30189180  2.00996883
Ti  0.89025912  1.61874725  0.63748068
```

13. Lattice geometry and ionic positions for  $\text{Ti}_{32}$  at 1500 K.

Format: XYZ file

```
50.0000000000    0.0000000000    0.0000000000
0.0000000000    50.0000000000    0.0000000000
0.0000000000    0.0000000000    50.0000000000

Ti -2.27607051  6.65628630 -1.28894540
Ti -0.77314793  2.36553055 -2.25649551
Ti  2.62750668 -0.04405092 -2.21442525
Ti  2.78911408 -0.14272941  2.49583016
Ti -2.27341289  4.64548915 -3.38156794
Ti  0.40917868  0.26122250 -3.73035839
Ti  2.64269200  1.54525732 -4.33059998
Ti -0.98542374 -1.44790425  0.45441938
Ti -2.01945058  2.21833258 -4.52285249
Ti  4.30066655 -0.75343502  0.08475329
Ti  1.77036986  2.73037575 -2.18868869
Ti -2.17780346  3.96984985 -0.66164957
Ti  2.79324119  1.51004990  0.02001613
Ti  0.62600922 -1.92656843  2.64431148
Ti  0.07866114  0.92427587  2.08116704
Ti  0.61833892 -3.71470312  0.49223052
Ti -0.76567399  5.72624371  0.96667314
Ti  2.99212083 -2.71618869  1.67517354
Ti  0.37884589  0.48732877 -0.96866767
Ti -2.07450993  1.09208116  0.43768859
Ti -3.45245964  2.17159969 -2.33030325
Ti -4.48131561  2.73152040  0.25298750
Ti  1.59895467 -1.07438406  0.26456475
Ti  0.54511265  3.24261517 -4.66619758
Ti  0.22445026  4.96006417 -1.59954121
Ti -4.61406916  5.12448543 -1.34456859
Ti  0.58548779 -1.94272393 -2.04601630
Ti  3.04795974 -2.78920354 -1.10311445
Ti -1.50880588  3.19217231  1.93710954
Ti  0.43264195  2.99646357  0.14568052
Ti -3.50154541  5.13700465  1.17594463
Ti -1.89456264 -0.06308408 -2.45057982
```

14. Lattice geometry and ionic positions for  $\text{Ti}_{32}$  at 1600 K.

Format: XYZ file

```
50.0000000000    0.0000000000    0.0000000000
0.0000000000    50.0000000000    0.0000000000
0.0000000000    0.0000000000    50.0000000000

Ti  0.30872785   1.00205901  -2.88841271
Ti  1.83909784   3.60631425  -2.85256974
Ti  1.46656123   5.46391534  -4.55647656
Ti  -4.84107354  -1.29559858   0.99390362
Ti  2.87834848   1.02533874  -3.58600189
Ti  -0.22997627  -2.24750394   0.65568809
Ti  -2.00600360   1.55788314  -1.65227896
Ti  -2.13502920   4.19107727  -0.89532443
Ti  -2.53763026  -2.09169785   2.52386785
Ti  -2.95093293  -2.63220603  -0.20763687
Ti  -0.69465556   0.13098653   2.57552367
Ti  3.67754685   3.79829772  -4.65503064
Ti  1.86029749  -0.65960796   1.38907288
Ti  -0.23295166   4.73367034   0.82800667
Ti  -4.07436183  -0.61689407  -1.72603554
Ti  0.23193959  -2.45713714   3.12772480
Ti  0.16167873   2.94338678  -0.95900597
Ti  -3.59541206   0.67185517   2.89407043
Ti  -2.51115356  -0.12585386   0.59816419
Ti  -1.51432958  -0.98463235  -2.16529019
Ti  -0.00282363   0.25274394  -0.26710425
Ti  3.49406590   5.71412176  -2.67124202
Ti  1.16128460   2.14911072   1.47625720
Ti  2.40807628   1.39798452  -0.93230355
Ti  1.62428190  -1.22656348  -1.81486538
Ti  0.81639692   5.55278350  -1.54634072
Ti  4.36471193   2.99500704  -2.09848570
Ti  -0.92709359   3.64342098  -3.32652825
Ti  2.68282192   4.02553335  -0.13119246
Ti  -4.39448233   1.62343190   0.02315511
Ti  1.01051063   2.53720679  -5.14708851
Ti  -1.67533783   2.39483983   1.03775796
```

15. Lattice geometry and ionic positions for Ti<sub>32</sub> at 1700 K.

Format: XYZ file

```
50.0000000000    0.0000000000    0.0000000000
0.0000000000    50.0000000000    0.0000000000
0.0000000000    0.0000000000    50.0000000000

Ti  0.22133977 -0.46486036 -0.72720512
Ti -1.74521920 -0.02421044 -2.57399156
Ti -0.40280781  2.05916173 -1.72866598
Ti -1.60990075  3.45091807  0.36491517
Ti  1.90263550  5.83619006 -2.83691113
Ti -4.23346553  2.39485182  1.04698770
Ti -2.19537762 -0.48948949  4.21224424
Ti -0.51467777  4.61482181 -2.75779588
Ti -3.83458426 -0.43991883  1.91337835
Ti  3.78023634  1.26504708 -3.44173300
Ti -2.87532947  2.49386939 -2.11635472
Ti  2.65780406  6.56504713 -5.19781430
Ti  1.26514033  0.31466156 -3.17902568
Ti -2.29013202  1.56103163  2.77238578
Ti -0.00096650 -1.88731603  3.85910006
Ti -0.72208352  2.24333437 -4.38185628
Ti  0.49127297  0.61908565  3.65284991
Ti  1.10431613  4.16135524 -0.48479022
Ti  3.53266769  3.80136523 -1.41868736
Ti  2.27038150  1.50878062 -1.01240538
Ti  2.17397574  2.02291499 -5.47304573
Ti -2.09426103  0.83965505  0.06146648
Ti  1.09960270  4.48755655 -5.32777808
Ti -2.22117927 -2.79681969  2.77132924
Ti -0.94338177 -0.64538336  1.79851911
Ti  0.38293672  1.74021798  0.98485340
Ti  0.00899209 -2.85499666  1.10517572
Ti -4.20520854 -0.10537530 -1.50199562
Ti  3.77328740  4.35060027 -4.40934920
Ti  1.69496070 -0.65074958  1.39466655
Ti  1.71475175  3.00237578 -3.06594067
Ti -2.52262558 -1.90044891 -0.25854770
```

16. Lattice geometry and ionic positions for Ti<sub>32</sub> at 1800 K.

Format: XYZ file

```
50.0000000000    0.0000000000    0.0000000000
0.0000000000    50.0000000000    0.0000000000
0.0000000000    0.0000000000    50.0000000000

Ti  3.80323296  3.43989446 -2.99144545
Ti  0.43508932 -0.59007861  1.24348692
Ti  2.94941260  0.35577585 -3.44172976
Ti -0.73331889  4.19733040 -0.43960134
Ti -5.42603798  3.42025731 -0.31415477
Ti -1.71728822  2.93464468 -2.84670036
Ti  2.00100553 -0.00467876 -0.92238140
Ti  1.19946771  2.50489047 -2.60549732
Ti -0.35935678  1.60950263 -0.75603711
Ti  1.63368206  1.79672296  1.46217997
Ti  4.57631291 -1.24669168 -0.68841687
Ti -4.99759445  0.75907862 -0.84565606
Ti  5.22280111  1.11975346 -2.39425007
Ti -3.23944617  5.00183917 -0.91771869
Ti -0.25442503 -1.51208708 -1.13920281
Ti  2.18918217 -1.97824970 -2.55957539
Ti  2.09199989 -2.56199088  0.27365922
Ti -7.14603396  2.09431467 -1.75578955
Ti -6.95125131  1.51049630  0.73788772
Ti -2.90511317  3.97782094  1.65310714
Ti  5.93249452  3.43158216 -1.42070830
Ti  2.01481984  4.39311171 -1.07249773
Ti  3.34113123 -0.12621799  1.35881181
Ti -4.32527943  2.87870296 -2.55756641
Ti -2.96767245  2.32796426 -0.37655521
Ti  5.93720409  1.29328756  0.13853134
Ti -4.13885826  1.58081325  1.68304848
Ti -2.51367419 -0.15775585  0.12953541
Ti  3.58761427  2.22717563 -0.64072884
Ti -2.51042070  0.25688678 -2.55477413
Ti  0.18177715  0.10903920 -3.26578627
Ti -1.24835562  2.03013850  1.87050394
```



17. Lattice geometry and ionic positions for  $\text{Ti}_{32}$  at 1900 K.

Format: XYZ file

```
50.0000000000    0.0000000000    0.0000000000
0.0000000000    50.0000000000    0.0000000000
0.0000000000    0.0000000000    50.0000000000

Ti  0.31940411 -1.26185027  3.79255998
Ti  0.52279901  5.01553086 -3.77210969
Ti  1.63617818  0.65671031 -2.02507403
Ti  0.10582176  1.32113433  2.34922812
Ti -3.88375337 -0.92604003  1.51674784
Ti  3.12599004  3.59144295 -2.48367111
Ti  0.40506843 -3.47539018  2.02474321
Ti -1.35665267 -5.25872611  2.83294983
Ti  1.94689670  2.65220195  0.06951864
Ti -0.94664603  0.86898715 -3.11976303
Ti  1.32369540  5.16586425 -0.71173470
Ti -0.99479268  5.62064040 -1.44063627
Ti -0.38663507  1.00544283 -0.33243292
Ti  0.19926370  4.41522237 -6.30241665
Ti -1.35631103  3.24733604 -4.13977687
Ti  2.70098311  4.52246986 -5.30979803
Ti  0.62258105  7.57249518 -2.66002737
Ti -2.42181658  2.50702975 -0.99120268
Ti  1.51680477  2.13723001 -4.35798508
Ti -0.45377311  3.60328382  0.80425807
Ti  0.39561720 -3.34121875 -0.60371879
Ti -2.24127934 -0.22080007  3.81106599
Ti  0.33060140  3.14784315 -2.13219358
Ti -2.09200710 -3.37781526  0.77625279
Ti  3.09515633  6.31797442 -3.18654826
Ti  1.31220207  6.99741731 -5.02947650
Ti -2.11520680 -2.98718575  3.79530282
Ti -2.71508054 -0.38124638 -0.78549647
Ti -2.56611306  1.28703727  1.40069191
Ti -1.27516962 -1.01138456  1.54574797
Ti  1.40261780 -1.04281452  0.55144576
Ti -0.49334332 -1.29554895 -1.84247278
```

18. Lattice geometry and ionic positions for Ti<sub>32</sub> at 1941.15 K.

Format: XYZ file

```
50.0000000000    0.0000000000    0.0000000000
0.0000000000    50.0000000000    0.0000000000
0.0000000000    0.0000000000    50.0000000000

Ti  1.90087119 -3.67982871  2.41172697
Ti -2.39211734  4.79787051 -0.62959978
Ti -3.54429929  5.96273005 -2.93407354
Ti -0.95932292 -2.82419881  3.13734947
Ti -1.06604402  2.14895515 -4.12152407
Ti -2.59059968  4.44332694 -5.04715162
Ti -2.70939754  1.97790121  0.15774545
Ti -1.62437783  7.00712537 -4.51950326
Ti -3.24340234  2.95909168 -2.79588507
Ti -0.60540023  2.73158875  1.51820155
Ti -0.00128007 -1.51101873 -1.41756381
Ti  1.67537456  3.67208717 -2.83107986
Ti -0.11623609  0.63175884 -0.16047466
Ti -2.07031082  0.49533857 -2.00046463
Ti  1.22520538 -1.09793284  3.96489061
Ti  3.28728463 -1.37799488  2.03065386
Ti  2.02868320  2.31924380 -0.35267567
Ti -2.10171142 -1.41183030  0.11876167
Ti  1.79849754  1.02392995  1.87499697
Ti  1.95750171 -3.16354304 -0.38924321
Ti  0.87308308  6.26858284 -3.49319314
Ti -1.18027018  4.81698017 -3.10622409
Ti  2.36348418 -0.57545222 -0.66290283
Ti  4.41479519 -3.60903960  0.84418521
Ti -0.71969426  2.69876400 -1.62567284
Ti -0.57049752 -3.52925068  0.25258439
Ti -1.30570078  7.04042023 -1.56921553
Ti  0.89982383  0.87669402 -2.74198967
Ti -1.27613074 -0.04364784  2.43234712
Ti  0.41302347  4.26868815 -5.04843186
Ti  0.59490786 -1.51091515  1.38779340
Ti  0.30735800  5.26684877 -0.64038941
```

19. Lattice geometry and ionic positions for Ti<sub>32</sub> at 2000 K.

Format: XYZ file

```
50.0000000000    0.0000000000    0.0000000000
0.0000000000    50.0000000000    0.0000000000
0.0000000000    0.0000000000    50.0000000000

Ti  1.52050722 -1.20109972  1.29003469
Ti  5.07163847  1.68205488 -0.82041216
Ti  1.95364933 -2.68916844 -2.82071077
Ti -2.56187883 -1.00074438 -1.56408223
Ti  2.76310454  1.18109195  0.40542348
Ti  3.15236748 -0.76694933 -1.45920741
Ti  1.20713192  4.62394776 -3.02637820
Ti -4.77525292  1.22962567 -2.17496589
Ti  2.51362359  2.38729886 -1.85116159
Ti -1.33653318 -0.72532225  0.65090468
Ti -0.07441413  3.28850250 -1.04358302
Ti  0.76047534  0.45188978 -0.94323912
Ti -2.80616046  2.88683200 -3.22109629
Ti  1.58609225  5.22651431 -0.48115169
Ti  1.68432818  3.39738282  1.24940603
Ti -5.30117412  0.42098659  2.38061779
Ti -4.26730427 -0.58637454  0.25190925
Ti  2.36151331  3.05654525 -4.50851012
Ti -3.59650415  2.08602767  1.12943190
Ti  3.72570586  4.91423702 -2.81837209
Ti -3.91020164 -2.12431772  2.37437055
Ti -3.95251478  3.61158862 -0.93455380
Ti -2.48398255  0.23370783  2.56976025
Ti -0.02670070  1.51439641  1.62473880
Ti  0.20235002  1.59717891 -3.31763916
Ti -5.98811980  1.72689721 -0.09201773
Ti  0.49693339 -2.08973919 -0.74971287
Ti -1.81846406  4.12385479  0.72763746
Ti  2.50973815  0.40943792 -3.91208567
Ti  4.25225808  4.14520353 -0.29417846
Ti  4.83626817  2.63665623 -3.37787666
Ti -2.03537898  1.42513044 -1.19932181
```

20. Lattice geometry and ionic positions for Ti<sub>32</sub> at 2100 K.

Format: XYZ file

```
50.0000000000    0.0000000000    0.0000000000
0.0000000000    50.0000000000    0.0000000000
0.0000000000    0.0000000000    50.0000000000

Ti  1.95425996 -1.53934485 -3.02270161
Ti  2.57417095 -0.08209874  1.77648621
Ti  3.82709799 -2.58466259  1.00696054
Ti  3.19742165  2.61187919  1.47361879
Ti  2.67725159 -1.02006122 -0.75812675
Ti  3.82929286  1.52861162 -1.15980446
Ti -5.71347681  3.61371395 -0.50089199
Ti -3.15014219  5.13896618 -4.31790786
Ti  0.98343653 -3.33791890 -0.91824886
Ti  2.47557826  4.46770602 -0.73375590
Ti -3.66868094  1.72944332 -0.41897863
Ti  0.11530629  0.80805752 -2.43333153
Ti -4.72361156  2.59625259 -2.76029466
Ti -5.08957555  2.46195384  2.00101959
Ti -2.72422776 -0.89928723 -0.43670694
Ti -4.86831920  5.10765046 -2.72367391
Ti  5.10095858 -1.88481794 -1.58203642
Ti  4.78750893 -0.17319935  0.51581081
Ti  3.30075257 -3.72024680 -2.07583569
Ti  1.22537736  3.23330697 -2.56977840
Ti  1.34997264  1.69746665 -0.33253240
Ti  0.00326769 -0.72491868 -0.00395349
Ti -1.77445290  5.80100981 -2.24995052
Ti  1.01008046  4.23474656  1.82130138
Ti  0.02751895  4.55092281 -0.50711478
Ti -2.60681233  0.41669784 -2.73139827
Ti -0.70971740 -1.85607670 -2.35680874
Ti -3.29262761  4.81370642 -0.40169263
Ti -1.89890276  3.07456353 -2.76894133
Ti -1.16012491  1.99573667 -0.53264641
Ti -1.52439478  3.55713790  1.68136009
Ti  0.12891417  1.45637652  2.06453291
```

21. Lattice geometry and ionic positions for Ti<sub>32</sub> at 2200 K.

Format: XYZ file

```
50.0000000000    0.0000000000    0.0000000000
0.0000000000    50.0000000000    0.0000000000
0.0000000000    0.0000000000    50.0000000000

Ti 15.17694595 12.28030204 19.00113839
Ti 10.77186367 10.56844640 17.00039658
Ti 12.89548441 18.17038072 17.32182090
Ti 13.29415259 12.63758982 12.82071943
Ti 10.72878037 15.61971545 21.73165821
Ti 13.36112496 11.54356370 20.95030571
Ti 13.38686866 10.90352685 15.10944975
Ti 10.52964675 14.56568189 18.99195819
Ti 10.59200921 12.96200331 21.72465883
Ti 13.13048546 15.59108689 15.49300724
Ti 11.54264356 13.46516966 14.61001668
Ti 10.88867326 15.83568318 14.22602440
Ti 13.20414299 16.84968728 20.75505680
Ti 12.07646406 8.96058682 18.60327225
Ti 13.06360646 11.07355997 17.69427972
Ti 10.86110999 17.65529660 19.93145772
Ti 14.73305741 14.76223041 17.36542519
Ti 10.29742311 16.08693749 16.94815194
Ti 12.58393286 13.43396822 16.92914512
Ti 12.69309953 15.86239656 18.10596107
Ti 10.62733455 18.28810246 15.14779057
Ti 15.11401361 17.08579630 16.38056171
Ti 15.71183839 13.05265749 22.04647383
Ti 14.86206862 13.13196803 14.90911480
Ti 15.53298375 15.47133300 19.94413075
Ti 7.47873195 16.17665500 17.47533531
Ti 11.22255950 12.02944573 19.19218746
Ti 9.29470503 13.18882494 16.37121206
Ti 13.43484789 14.11105021 20.00376312
Ti 13.71473619 14.78645366 22.61011876
Ti 11.63450633 9.81043922 21.12729384
Ti 11.22325966 11.11273407 13.52209179
```

22. Lattice geometry and ionic positions for Ti<sub>32</sub> at 2300 K.

Format: XYZ file

```
50.0000000000    0.0000000000    0.0000000000
0.0000000000    50.0000000000    0.0000000000
0.0000000000    0.0000000000    50.0000000000

Ti -2.88206330  1.23859922 -1.19661742
Ti -0.90052964 -1.91380674  1.67057149
Ti  2.48103754  3.00074503 -2.29227809
Ti  0.60252428  4.46840189 -4.09339670
Ti -1.56085627 -1.86236224 -0.90736412
Ti -0.31645468  2.30874574 -2.14859575
Ti  1.32743799 -2.39674467  0.12550111
Ti -2.50430851  4.82515309  1.93925428
Ti -1.13032845  0.28825237 -3.89133345
Ti -0.97283151  2.72539701 -5.02560675
Ti -1.61116796  4.58721296 -2.55485691
Ti  0.56773460  4.92960788  1.48548482
Ti  3.42959771 -0.08882420 -3.10289029
Ti -1.28299391  3.20812289  0.11966189
Ti  0.92407239 -1.77059411 -4.41172018
Ti  0.63413029  4.95326081 -1.38681681
Ti -2.24684362  0.73884205  2.02539621
Ti  1.50344596  1.37772645 -4.10526342
Ti -3.86848022  4.17786339 -1.11348511
Ti  2.06443211  1.91744854  3.53992198
Ti -4.03149240  2.55426421  1.11219141
Ti  2.74029695 -0.15248290  2.22297901
Ti  1.36535737  2.79739627  0.52102374
Ti  0.25287198 -0.17555557  3.71226856
Ti  2.99914145 -2.54801853 -1.98694930
Ti  0.61384140 -0.39385775 -2.18779135
Ti  2.61501209  0.35965190 -0.72151042
Ti  0.03931858 -3.59356287 -2.55143877
Ti  0.17496046  0.11840275  0.71594807
Ti -0.50473126  2.74611323  2.61575668
Ti -3.15093734  2.55478593 -3.70073128
Ti -1.70809333  6.09308935 -0.38333499
```

23. Lattice geometry and ionic positions for Ti<sub>32</sub> at 2400 K.

Format: XYZ file

```
50.0000000000    0.0000000000    0.0000000000
0.0000000000    50.0000000000    0.0000000000
0.0000000000    0.0000000000    50.0000000000

Ti -20.89617835  14.26363588 -21.28528833
Ti -13.27304327   8.90971657 -19.35799602
Ti -18.99122224  14.49472705 -18.46473089
Ti -20.85738323  13.45212287 -23.77369397
Ti -19.56448613  12.03043406 -17.33927863
Ti -19.19194791  12.31211883 -20.08080634
Ti -19.27483409  14.16463143 -15.47524033
Ti -14.87828027  11.21300929 -17.31115377
Ti -17.29771800  10.16658595 -21.47863410
Ti -16.01228387  14.39541866 -19.36399669
Ti -21.90314167  12.93153566 -18.71165935
Ti -17.28983380  16.30241771 -17.35038004
Ti -13.51572443  10.69884261 -21.42862407
Ti -15.72318109  12.31513733 -22.21781654
Ti -18.14896820  14.69665817 -21.22319757
Ti -14.48670484  15.73898669 -15.79938808
Ti -17.90800677  16.79206961 -19.60847566
Ti -14.99898818   8.68406769 -21.10856587
Ti -14.75569359   6.60251189 -19.61434294
Ti -18.81247255  12.36103947 -22.72178891
Ti -16.09815233   9.14575238 -19.04135546
Ti -22.17277824  11.64158103 -22.55883961
Ti -16.48532225  11.87635667 -19.57961291
Ti -14.84651297  17.09976598 -18.09152058
Ti -16.60851169  13.53688234 -16.46031017
Ti -13.88774897  14.01560831 -17.52778676
Ti -12.90644284   7.25200457 -21.85427411
Ti -17.66755965   7.54840945 -20.83623678
Ti -21.00869177  16.27026029 -19.14888527
Ti -21.49559567  14.64813122 -17.06336590
Ti -13.78254926  12.20178613 -19.17745017
Ti -19.59694117   9.31106757 -20.90132607
```